

Evaluation of the Residual Stress State of 42crmo4 Steel Sheets in a Production Line

Allan Romário de Paula Dias^{a*}, Rafael Menezes Nunes^a, Toni Roger Schifelbain de Lima^a,

Thomas Gabriel Rosauro Clarke^a

^aPost-Graduation Program in Mining, Metallurgical, and Materials Engineering - PPGE3M, Federal University of Rio Grande do Sul - UFRGS, Av. Bento Gonçalves, 9500, prédio 104, CEP 91509-900, Porto Alegre, RS, Brazil.

Received: February 3, 2015; Revised: September 5, 2015; Accepted: November 26, 2015

The residual stress state of a mechanical component is an important factor in its production planning and in estimates of its lifecycle since it can be responsible for geometric distortions and degradation of fatigue properties. Therefore, the development of reliable methods for non-destructively quantifying these stresses remains in the interest of most manufacturing industries; Barkhausen magnetic noise measurements have been investigated in several applications and remains a viable option. However, its effective implementation has occurred mostly in components with simple geometries and insignificant microstructural gradients; even in these cases, successful industrial adoption of the method depends on previous calibration with samples that are often difficult and costly to prepare and validate. This work aims at investigating the capability of the method of characterizing the residual stress state in a simple but generally useful application: samples of hot-rolled steel sheets collected at two different stages of processing in an industrial mechanical conformation and heat treatment plant. In this analysis Barkhausen noise measurements were compared to X-ray diffraction results, and statistical analysis tools were used to correlate the results.

Keywords: Residual stresses, Barkhausen noise, X-ray diffraction, Steel sheets

1. Introduction

There is a consensus among researchers that no mechanical component is free from residual stresses¹, since these are introduced in the object every time a process causes temperature, deformation, or phase transformation gradients. Hence, fabrication processes such as mechanical conformation or heat treatment can lead to significant levels of residual stresses that in their turn can lead to premature failure, distortion, or even increases in corrosion rates when a component is deployed².

A number of methods aimed at inspecting and quantifying residual stress levels non-destructively have been proposed; many of these are based on measurements of electromagnetic properties³⁻⁵, Barkhausen noise measurements being recognized as one of the most promising alternatives.

Barkhausen noise arises from discontinuities in the dynamics of magnetic domain motion when a material is subjected to magnetic fields. It arises from sequential bursts of energy emitted when domain boundaries are set free from microstructural barriers that temporarily obstruct the process of orientation of domains in the direction of an imposed magnetic field⁵. Analysis of the noise signal generated during magnetization of the material allows it to be correlated to local residual stress levels, among other material properties⁶. The signal is usually captured by a sensor coil positioned in the vicinity of the region of the component being subjected to magnetization, and it is intimately related to the microstructural condition of the material⁷, its plastic deformation level⁸,

and magnetostriction effects⁴. Once calibrated, it can be used to inspect a large number of components in a fast and reliable way, thus being ideal for production line quality control. However, the calibration procedure is usually the most time-consuming part of the inspection, because the operator needs to produce standards which isolate the effect being sought in the real component from other influences.

Magnetostriction is the common designation for the reciprocal effect between magnetization and strain in a material. When such a material is subjected to a mechanical load its magnetic domains will reorientate, and, in the case of ferrous alloys, align themselves in the direction of an imposed uniaxial stress⁵. As the stress state becomes more complex so does the magnetization behavior of the material. The phenomenon was described by Joule and Villari^{9,10} as set of equations:

$$\epsilon = S^H \sigma + dH \quad (1)$$

$$B = d\sigma + \mu^\sigma \quad (2)$$

In which ϵ is the strain, S^H is the compliance at constant magnetic field, σ is the stress, μ^σ is the relative permeability under stress, $d\sigma$ and dH are the infinitesimal variation of stress with magnetic induction and magnetic field with the strain respectively, and B is the magnetic induction¹¹.

In rolled ferromagnetic alloys the residual stress state usually means that magnetic domains will align themselves in the direction of easiest magnetization, which coincides with

*e-mail: allan.dias@ufrgs.br

the rolling direction¹². However, microstructure also plays an important role. In steels, ferrite, martensite, and bainite are all magnetic to different degrees, whereas austenite is not. A successful residual stress characterization technique should measure residual stress distributions independently, within an acceptable variability range regarding phase distribution, and should be able to discriminate between the two contributions.

This work aims at verifying the viability of the use of Barkhausen noise measurements to analyze residual stresses in 42CrMo4 steel hot-rolled sheets, under different microstructural conditions. This was done by comparison between X-ray diffraction results and Barkhausen noise measurements on samples extracted from two different stages of a production line, which involved different degrees of influence of straightening, heat treatments, and finishing processes.

2. Materials and methods

Samples of a DIN 42CrMo4 (equivalent to an AISI 4140 steel) plate which had been previously hot-rolled to a thickness of 2 mm and delivered in a coil were extracted directly from a production line. Samples were taken from two separate points along the production line so that two conditions were available: (i) uncoiled and straightened in a roll-type machine; (ii) uncoiled and straightened, austempered, tempered, and finished by superficial grinding. The first and second conditions are named HR and GR respectively in the rest of this paper.

Barkhausen noise measurements were taken along the samples as indicated in Figure 1. The sensor consists of a simple combination of a magnetization yoke and a pick-up Hall effect sensor. An alternated magnetic field is induced in the sample with the yoke, while the pick-up reads the response with lateral and longitudinal resolutions of 2mm and 3mm respectively. The sensor is connected to front-end electronics that provide variable excitation parameters, and are also responsible for data collection, storage and processing.

A 200 Hz sinusoidal excitation signal was imposed on the yoke, its amplitude being selected as to maximize the signal-to-noise relation, the only limitation being that the material remained below the previously determined magnetic saturation of the material. This excitation frequency was selected during a previous parametric study, which showed the highest response at this value. Band pass filters in the 1-5MHz range were used in order to limit the measured noise to high frequencies, so to guarantee that the Barkhausen emissions

registered were isolated from the excitation signal and any of its stronger harmonics and these values are confined in the region between 2 – 10 μm ^{13, 14}. More importantly, this frequency range was chosen as to limit the depth of the Barkhausen emissions being collected by the pick-up to values similar to those of the XRD analysis¹⁵.

The XRD measurements were taken at the same positions as shown in Figure 1. The equipment used was a GE Seifert Charon XRD M – Research Edition, in a ψ -configuration (lateral inclination) and Bragg-Brentano geometry, equipped with a Cr-K α radiation with a Vanadium filter. A primary spot size of 2mm in diameter and a linear detector with 20° range (GE Meteor 1D model) were also used.

The diffraction line corresponding to the (211) plane at 156.08° was used for residual stress calculation. Hence, a 2θ scan range from 148 to 165° was chosen, with a 0.05° step and a 10s time step. These scans were made at each of 11 side inclination angles between $\pm 60^\circ$ in the ψ -direction. PLA corrections and separation of K α 1 and K α 2 parts of diffraction lines has been applied. Linear background was determined by 5 measured data points on right and left side of each recorded diffraction line and was subtracted from maximum intensity. The sliding gravity method used the calculation of gravity centres for 8 different levels (10 to 80% in steps of 10%) of maximum peak intensity, subtracted by background intensities. Strains of these 8 different calculations are weighted by the standard deviation of individual data points from the linear regression and with the X-ray elastic constants are converted to a residual stress value. Secondly the fit procedure used the maximum of the Pseudo-Voigt function as a possible value for peak positions, and again with the slope of the regression line and the XEC's a residual stress was calculated¹⁶. This is critical in order to calculate the residual stresses with the $\sin^2\psi$ method, with the mechanical properties and parameters shown in Table 1. Values of full width at half maximum (FWHM) were also extracted for each measurement point.

Because of restrictions in the size of the samples that could be analyzed in the XRD equipment, samples had to be kept to a maximum of 300mm in length, whereas the original samples were 3 times this length. A preliminary study showed that cutting the samples relieved residual stresses up to 50mm from the cut edges. Therefore, only measurements taken in the region that was not affected by the cutting procedure are considered in the following figures, but results are showed continuously for the entire length of the original samples (750mm).

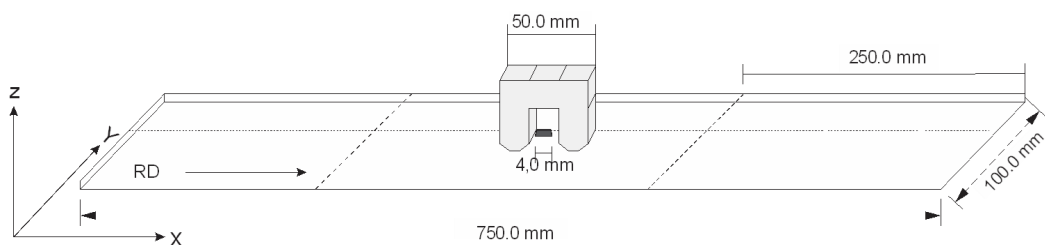


Figure 1. Schematic showing the position and direction of Barkhausen noise measurements along the steel sheet samples, and at the center of its width.

Table 1. Mechanical properties and parameters used to determine the residual stress values at each point with the $\sin^2\psi$ from recorded diffractograms.

Parameter	Symbol	Value
Angle range	θ	148 – 165°
Step	θ	0,05 °
Time step	t	10 s
Young's modulus	E	212 GPa
Poisson's ratio	ν	0,28
-S ₁ Constant	-S ₁	-1,237x10 ⁻⁶ MPa
½S ₂ Constant	½S ₂	5,709x10 ⁻⁶ MPa

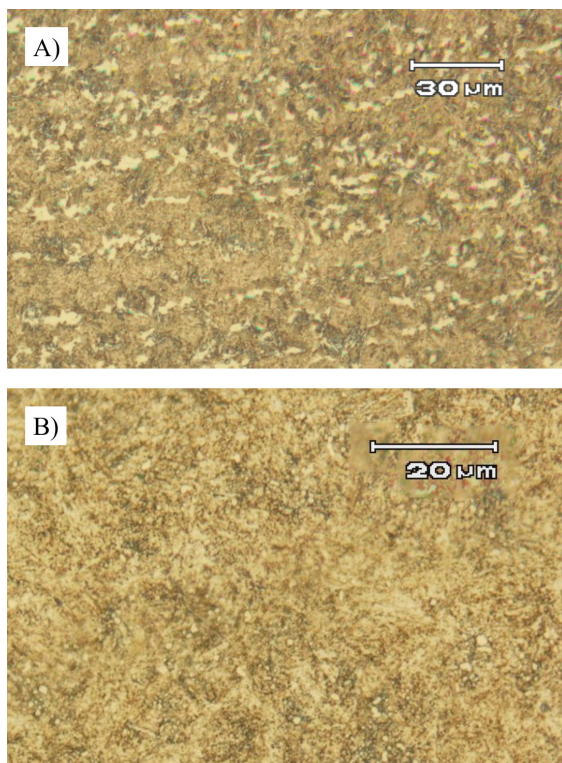


Figure 2. Microstructure of samples in conditions: a) HR (uncoiled and straightened); and b) GR (uncoiled, straightened, austempered, tempered, and surface finished). Images obtained from optical microscopy and etching with Nital 2%.

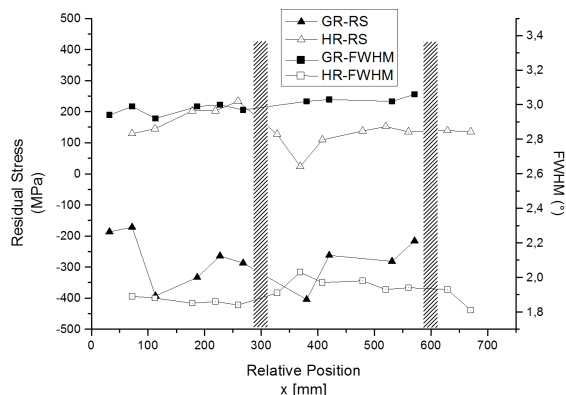


Figure 3. Residual stress and FWHM profiles measured along the longitudinal ("x") direction for GR and HR samples.

3. Results and discussion

Initially, metallographic analyses of the samples were performed in order to determine their phase distribution. Figure 2 shows that samples in HR condition (uncoiled and straightened) were Ferritic - Perlitic with some dispersed carbides. Samples in condition GR had a typical microstructure of tempered martensite, with a high density of carbides in a Ferritic matrix.

Samples were then characterized by XRD along a line at the centre of their width as shown in Figure 1. Results are shown in Figure 3 along with values of FWHM (Full width at half maximum), which can be related to second order residual stresses; these can be traced to deformations of the lattice, and can be related to processes that generate localized plastic deformation or distortion in the component.

In GR samples, residual stresses are compressive and vary in the range of -200 to -400 MPa with a significant dispersion in the results. The average FWHM is of 3.1°. For HR samples, tensile stresses in the order of 200 MPa are seen, with less dispersion in the results. The average FWHM for these samples is 1.9°; the considerable difference in these values between the two conditions indicates that although the heat treatments and finishing processes are generating a more beneficial superficial residual stress condition for performance under fatigue (compressive stresses), they are also leading, as expected, to some distortion of the sheet.

Figure 4 shows a typical response signal for the Barkhausen measurements. The envelope of the Barkhausen noise emissions during magnetization of samples in GR and HR conditions is considered in this analysis. This is obtained by taking the local RMS value of the signal in a window of a predefined size. Differences in amplitude and in shape were seen in the signals for each of the conditions. This is due to a combination of the influences of microstructure and stress state. In terms of microstructure both materials have features that can act as barriers to magnetic domain motion: GR samples have small and dispersed carbides in a Ferrite matrix, whereas HR samples have smaller grains (and more grain boundaries) and interfaces between phases (fine perlite). It is difficult to estimate which of the microstructures has a more pronounced effect, especially since the stress state is considerably different.

A double-peaked noise emission curve is seen for HR, whereas a single peak of smaller amplitude is seen for GR. Some results in literature^{17, 18, 19} indicate that the shape of the curves may be more intimately related to the microstructure of the material rather than its residual stress state, although such assertions will be avoided in this case. It can also be seen in Figure 4 that amplitude values are higher for samples in the HR condition. This can be because the tensile nature of the longitudinal residual stresses in these samples creates a direction of relatively easy magnetization through the magnetostriction effect, increasing the energy with which domains move. In GR samples magnetostriction effects related to the compressive stresses seen in Figure 3, which interacts negatively with the easy magnetization axis, make magnetization harder in this direction, leading to the lower amplitudes seen in Figure 4.

Figure 5 shows the residual stress value determined by XRD compared to the amplitude of the RMS envelope of Barkhausen noise for each point on the samples. The correlation

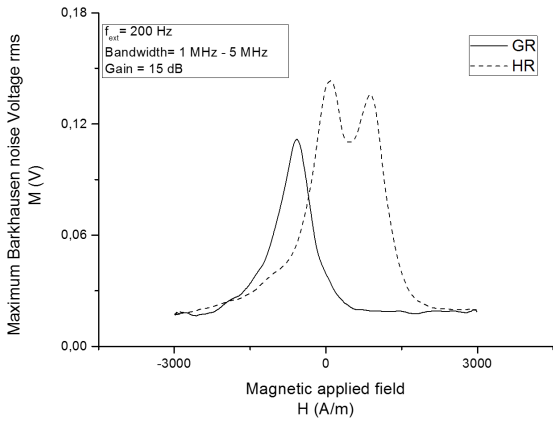


Figure 4. RMS envelope of Barkhausen noise for samples in HR and GR conditions.

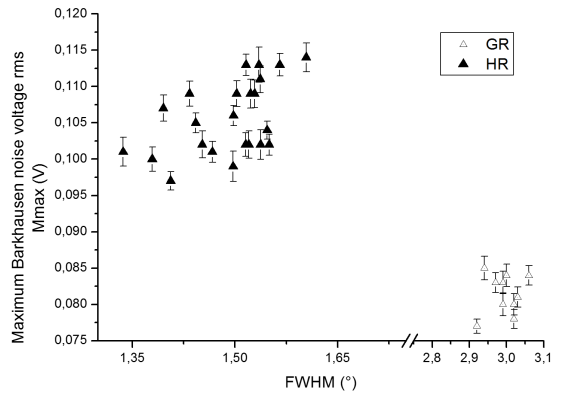


Figure 7. Correlation between FWHM values from XRD results and the maximum amplitude of the RMS of the Barkhausen noise signal.

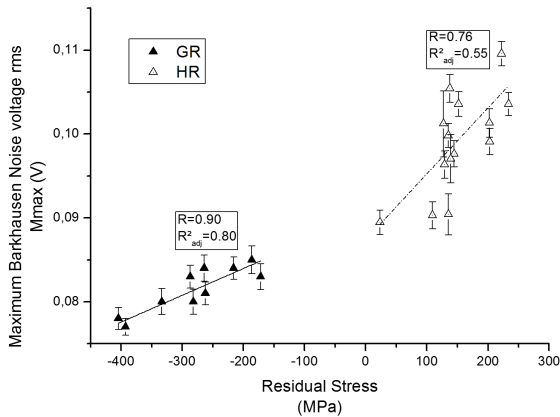


Figure 5. Correlation between XRD measured residual stress values and amplitude of the RMS of Barkhausen noise signals at each point on samples HR and GR.

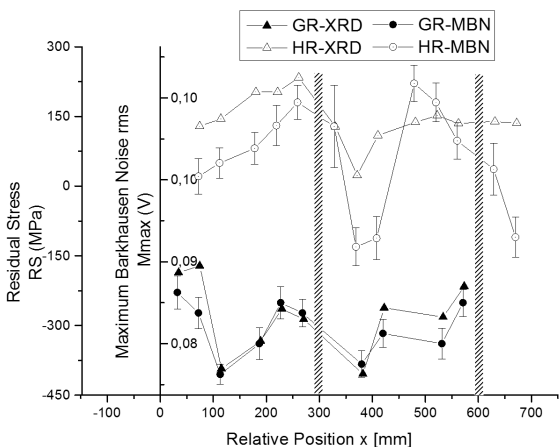


Figure 6. Comparison between XRD residual stress values measured along the longitudinal (“x”) direction and the amplitude of the RMS of the Barkhausen noise signal.

between XRD measured stress values and amplitude of the RMS of the Barkhausen noise was strong for samples in both conditions (as shown by R values of the fitted lines in Figure 5). The larger scattering of the points for samples in HR condition led to a lower R value. This may be caused by microstructural variations along the HR samples due to the straightening process, and was similarly seen in Figure 3 and verified by²⁰ in a study about the influence of pre-strain stress in MBN residual stress analysis. Such an effect is not seen in GR samples because these variations have been made more homogeneous with the heat treatments and, especially, the surface finishing process.

Figure 6 shows a comparison between the XRD measurements and the amplitude of the RMS of the Barkhausen signal along the longitudinal direction of the samples; a similar trend is seen for both curves and both conditions. This figure also shows that the scattering for HR samples is similar for measurements with both methods.

The heterogeneity of the microstructure in HR samples is corroborated by the larger dispersion in the values of FWHM in Figure 3. This is made more evident when FWHM values are compared to the maximum of the RMS envelope of the Barkhausen noise in Figure 7. Again, a strong dispersion is seen for HR values, indicating that plastic deformation occurred in a heterogeneous distribution along the sample, probably because of the straightening process and the lack of further heat treatment and finishing stages.

4. Conclusions

- In XRD measurements, uncoiled and straightened hot-rolled sheets showed considerable levels of tensile residual stresses along the rolling direction, with the high scattering in the measured values being attributed to the uneven deformation caused by the roll-type straightening machine that was used.
- The residual stresses became considerably compressive in the same sheets after they were austempered, tempered, and subjected to a surface

finishing process. Low scattering in the results suggests heat treatments and the surface finishing process were effective in removing the uneven deformation caused by the straightening process (in the near-surface region evaluated).

- The same XRD measurements showed a higher variability in FWHM values for the samples that were subjected to heat treatments and finishing processes, suggesting these led to distortion in the sheets.
- Barkhausen noise measurement showed good correlation with residual stress values obtained

through XRD measurements at the analyzed depths. Nevertheless, inhomogeneities dramatically affect the accuracy of the calibration and lead to difficulties in interpretation and contribute to a reduction in the reliability of the residual stress measurements.

- The influence of microstructure on the Barkhausen measurements is difficult to be isolated from the influence of residual stresses. Careful preparation and characterization of reference samples should be performed to gain more knowledge if commercial application is to be sought.

References

1. Totten GE, Howes MA and Inoue T. *Handbook of residual stress and deformation of steel*. Ohio: ASM International; 2002.
2. Schajer GS. *Practical residual stress measurement methods*. United Kingdom: John Wiley & Sons; 2013.
3. Abu-Nabah BA and Nagy PB. High-frequency eddy current conductivity spectroscopy for residual stress profiling in surface-treated nickel-base superalloys. *NDT & E International*. 2007; 40(5):405-418. <http://dx.doi.org/10.1016/j.ndteint.2007.01.003>.
4. Gorkunov ES, Subachev YV, Povolotskaya AM and Zadvorkin SM. The influence of an elastic uniaxial deformation of a medium-carbon steel on its magnetostriction in the longitudinal and transverse directions. *Russian Journal of Nondestructive Testing*. 2013; 49(10):584-594. <http://dx.doi.org/10.1134/S1061830913100057>.
5. Bozorth RM. *Ferromagnetism*. Piscataway: IEEE Press; 1993.
6. Kleber X, Hug A, Merlin J and Soler M. Ferrite-martensite steels characterization using magnetic barkhausen noise measurements. *ISIJ International*. 2004; 44(6):1033-1039. <http://doi.org/10.2355/isijinternational.44.1033>
7. Ktena A, Hristoforou E, Gerhardt GJ, Missell FP, Landgraf FJ, Rodrigues DL, et al. Barkhausen noise as a microstructure characterization tool. *Physica B, Condensed Matter*. 2014; 435:109-112. <http://dx.doi.org/10.1016/j.physb.2013.09.027>.
8. Hwang DG and Kim HC. The influence of plastic-deformation on barkhausen effects and magnetic-properties in mild-steel. *Journal of Physics. D, Applied Physics*. 1988; 21(12):1807-1813.
9. Joule JP. XVII. On the effects of magnetism upon the dimensions of iron and steel bars. *Philosophical Magazine. Series 3 (1832-1850)*. 1847;30(199):76-87. <http://dx.doi.org/10.1080/14786444708645656>.
10. Villari E. Change of magnetization by tension and by electric current. *Annual Physical Chemistry*. 1865; 128:87-122.
11. Olabi AG and Grunwald A. Design and application of magnetostrictive materials. *Materials & Design*. 2008; 29(2):469-483. <http://dx.doi.org/10.1016/j.matdes.2006.12.016>.
12. Stefanita CG. Barkhausen noise as a magnetic nondestructive testing technique. In: Stefanita CG. *From bulk to nano. The many sides of magnetism*. Berlin: Springer Berlin Heidelberg; 2008. p. 19-40.
13. Casavola C, Pappalettere C and Tursi F. Calibration of barkhausen noise for residual stress measurement. In: Ventura CE, Crone W, Furlong C, editors. *Experimental and applied mechanics*. New York: Springer Verlag; 2013. v. 4. p. 255-266.
14. Desvaux S, Duquennoy M, Gualandri J and Ourak M. The evaluation of surface residual stress in aeronautic bearings using the Barkhausen noise effect. *NDT & E International*. 2004; 37(1):9-17. [http://dx.doi.org/10.1016/S0963-8695\(03\)00046-X](http://dx.doi.org/10.1016/S0963-8695(03)00046-X).
15. Clarke DW and Hemp J. Eddy-current effects in an electromagnetic flowmeter. *Flow Measurement and Instrumentation*. 2009; 20(1):22-37. <http://dx.doi.org/10.1016/j.flowmeasinst.2008.09.002>.
16. Hauk V and Behnken H. *Structural and residual stress analysis by nondestructive methods. Evaluation, application, assessment*. Amsterdam: Elsevier; 1997.
17. Moorthy V, Vaidyanathan S, Jayakumar T and Raj B. Microstructural characterization of quenched and tempered 0.2% carbon steel using magnetic Barkhausen noise analysis. *Journal of Magnetism and Magnetic Materials*. 1997; 171(1-2):179-189. [http://dx.doi.org/10.1016/S0304-8853\(97\)00049-8](http://dx.doi.org/10.1016/S0304-8853(97)00049-8).
18. Vashista M and Moorthy V. Influence of applied magnetic field strength and frequency response of pick-up coil on the magnetic Barkhausen noise profile. *Journal of Magnetism and Magnetic Materials*. 2013; 345:208-214. <http://dx.doi.org/10.1016/j.jmmm.2013.06.038>.
19. Perez-Benitez JA, Espina-Hernandez JH, Martinez-Ortiz P, Chavez-Gonzalez AF and de la Rosa JM. Analysis of the influence of some magnetizing parameters on magnetic barkhausen noise using a microscopic model. *Journal of Magnetism and Magnetic Materials*. 2013; 347:51-60. <http://dx.doi.org/10.1016/j.jmmm.2013.07.034>.
20. Lindgren M and Lepisto T. Effect of prestraining on Barkhausen noise vs. stress relation. *NDT & E International*. 2001; 34(5):337-344. [http://dx.doi.org/10.1016/S0963-8695\(00\)00073-6](http://dx.doi.org/10.1016/S0963-8695(00)00073-6).